



Flow through a defective mechanical heart valve: A steady flow analysis

O. Smadi^a, M. Fenech^b, I. Hassan^a, L. Kadem^{a,*}

^a *Mechanical and Industrial Engineering, Concordia University, Montreal, QC, Canada*

^b *Mechanical Engineering, University of Ottawa, Ottawa, ON, Canada*

Received 20 November 2007; received in revised form 27 May 2008; accepted 1 July 2008

Abstract

Approximately 250,000 valve replacement operations occur annually around the world and more than two thirds of these operations use mechanical heart valves (MHV). These valves are subject to complications such as pannus and/or thrombus formation. Another potential complication is a malfunction in one of the valve leaflets. Although the occurrence of such malfunctions is low, they are life-threatening events that require emergency surgery. It is, therefore, important to develop parameters that will allow an early non-invasive diagnosis of such valve malfunction. In the present study, we performed numerical simulations of the flow through a defective mechanical valve under several flow and malfunction severity conditions. Our results show that the flow upstream and downstream of the defective valve is highly influenced by malfunction severity and this resulted in a misleading improvement in the correlation between simulated Doppler echocardiographic and catheter transvalvular pressure gradients. In this study, we were also able to propose and test two potential non-invasive parameters, using Doppler echocardiography and phase contrast magnetic resonance imaging, for an early detection of mechanical heart valve malfunction. Finally, we showed that valve malfunction has a significant impact on platelet activation and therefore on thrombus formation.

© 2008 IPEM. Published by Elsevier Ltd. All rights reserved.

Keywords: Mechanical heart valve; Defective leaflet; Doppler Echocardiography; Numerical simulations

1. Introduction

The aortic valve is located between the left ventricle and the ascending aorta. Its role is to open with minimal obstruction to flow during the ventricular ejection process: the systolic phase and to close with minimal leakage during the ventricular filling phase: the diastolic phase. Aortic stenosis (AS) is defined as the pathological narrowing of the aortic valve. In industrialized countries, AS is the most frequent valvular heart disease and the most frequent cardiovascular disease after systemic hypertension and coronary artery disease. When an AS is severe and the patient is symptomatic, aortic valve replacement is the only treatment that has been demonstrated to be efficient for patients to avoid

possible congestive heart failure and to improve heart performance. The native valve can be replaced by a biological valve (porcine valve or pericardial valve) or a mechanical valve. Approximately 250,000 valve replacement operations occur annually around the world and more than two thirds of these operations use mechanical heart valves (MHV) as a preferable choice [1]. This choice can be explained by the fact that mechanical valves have a longer lifespan when compared to biological valves. However, a patient with a mechanical valve must take anticoagulant medication life long because of risks of thromboembolic complications. Another potential complication associated with mechanical valves is valve malfunction (usually an incomplete opening of one or both leaflets in bileaflet mechanical valves) due to pannus (prevalence 0.14–0.65% patients/year [2]) and/or thrombosis formation. Although the occurrence of such malfunctions is quite low, however, they make the patient under a very high risk that requires an immediate surgery. Once the obstruction becomes severe, cinefluoroscopy or computed tomography can be used to confirm restricted motion of one

* Corresponding author at: Laboratory for Cardiovascular Fluid Dynamics, Department of Mechanical and Industrial Engineering, Concordia University, 1455 de Maisonneuve Blvd W, Montreal, QC, Canada H3G 1M8. Tel.: +1 514 848 2424x3143; fax: +1 514 848 3175.

E-mail address: kadem@encs.concordia.ca (L. Kadem).

or two leaflets of the prosthesis. Unfortunately, due to risk associated with X-ray exposure, these methods cannot be used for the routine follow-up of patients with prosthetic valves. It is therefore essential to develop and validate screening non-invasive methods for early detection of prosthetic valve malfunction. However, distinguishing between a normal and a dysfunctional bileaflet mechanical valve, especially when only one leaflet is blocked, using a non-invasive technique such Doppler echocardiography, is a complex problem since (1) as a result of acoustic shadowing from the sewing ring, it can be difficult to image the valve and detect if the leaflets are working properly, (2) transvalvular pressure gradients may be overestimated by Doppler echocardiography due to the recording of localized high gradient. In this situation, it is difficult to determine if the high gradient is due to an intrinsic dysfunction of the prosthesis or to a localized benign phenomenon due to the specific geometry of bileaflet mechanical valves [3].

It is, therefore, essential to develop new non-invasive parameters allowing an accurate and an early detection of mechanical valve malfunction. Furthermore, these parameters should be flow independent to be applicable to a large number of patients.

For this purpose, we elected, as a first approach, to perform numerical simulations of a continuous flow through a defective mechanical valve under several flow conditions and for different malfunction severities. This is the first numerical study dealing with mechanical valve malfunction with as a main objective determining a non-invasive parameter able to early detect if one valve leaflet is blocked. It should be noted that the current study focuses only on one blocked leaflet, since this case is more complex to be detected when compared to the case where both leaflets are blocked [4]. In vitro the flow through a defective CarboMedics mechanical bileaflet valve was only studied by Baumgartner et al. [5] with as objective showing the discrepancy between catheter and Doppler pressure gradients. They showed that this discrepancy, that usually happen in normal bileaflet valves, decreases with defective leaflets due to energy losses (i.e. friction, flow separation and vortex formation) which lead to noticeable reduction in pressure recovery downstream of the valve. As a result, underestimation for real hemodynamic changes might occur and the clear definition for normal and abnormal flow will be difficult.

The objectives of this study are, therefore, to describe the flow dynamics through a bileaflet mechanical aortic valve with one immobilized leaflet from fully opened (0% malfunction) to fully closed (100% malfunction) position and to find a suitable method of predicting the malfunction by using an non-invasive parameter, that can be measured by Doppler echocardiography or magnetic resonance imaging. We will also investigate the potential clinical complications in terms of platelets activation and red blood cells damage associated with a defective leaflet in a bileaflet mechanical valve.

2. Models and methods

To investigate the flow through a defective mechanical valve, five 2D models were created in the current study. The lower leaflet was moved from fully opened position (85° ; 0% malfunction) to fully closed position (30° ; 100% malfunction) with three equally spaced intermediate angles of 71.25° (25% malfunction), 57.5° (50% malfunction) and 43.75° (75% malfunction). As shown in Fig. 1, non-symmetric sinuses were modeled based on the in vivo study performed by Reul et al. [6] and used in vitro by Grigioni et al. [7]. For the upstream and downstream sections, the inlet section was 15 mm upstream from the valve and the outlet section was 85 mm downstream of the valve. The bileaflet mechanical valve was modeled based on a 25 mm St. Jude Medical Hemodynamic Plus valve. Therefore, the inner diameter was 22.3 mm and the outlet diameter was 32.3 mm. The hinge mechanism of the valve has been neglected and this valve has been chosen since it is the most commonly implanted clinically.

For all the above mentioned severities, several systolic flowrates have been simulated: 7.5, 10.5, 15, 18 and 21 L/min, which represent a cardiac output of: 2.5, 3.5, 5, 6 and 7 L/min, respectively. This will simulate normal and strenuous exercise conditions. For blood properties, we considered the common values for density and dynamic viscosity which were equal to 1000 kg/m^3 and 0.0035 kg/m s , respectively. Under these conditions, the Reynolds number ranged from 2038 to 5708 based on average inlet velocity, inlet diameter and the viscosity of the fluid. This range of Reynolds number reasonably represents the turbulent nature of the flow downstream of the valve [8,9].

Fluent 6.3.26 (Fluent Inc., Lebanon, NH, USA) commercial software based on finite volume method was used to run the numerical simulations. Due to the absence of a numerical method able to describe the complete physiological flow and

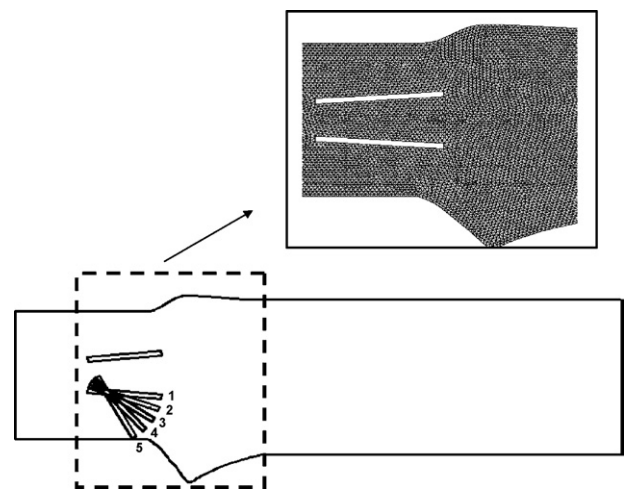


Fig. 1. Model geometry for the five different cases; (1) 0% malfunction; (2) 25% malfunction; (3) 50% malfunction; (4) 75% malfunction; (5) 100% malfunction (Mesh quality for the sinuses and leaflets is also shown).

the need to simulate flow near and during the peak systolic phase to assess the level of clinical complications, the flow was assumed steady, turbulent, and Newtonian. In this study, standard k-ε model was used with 5% of turbulent intensity and 22.3 mm as hydraulic diameter [10,11]. Mesh independency was achieved using 37,232 elements in all cases. The wall shear stress and velocity profiles across the valve at different positions downstream of the valve (0.5D, 1D and 2D) and also the maximum velocity value and position were used to check the mesh independency.

For the boundary conditions, total pressure was considered as inlet condition and was changed with each case until the desired flow rate was reached. Zero static pressure was used as outlet condition, and no slip condition was used at the solid walls.

3. Results

3.1. Velocity distribution and profiles

Figs. 2 and 3 show the velocity contours for the entire field for different percentages of valve malfunction at flow rates equal to 5 and 7 L/min, respectively. Due to the differ-

ence in leaflet opening angles, the flow patterns developed upstream and downstream of the defective valves were different from healthy ones. In general, flow separation and vortex formation were noticed in all cases. In Fig. 2, for $Q=5$ L/min, the maximum velocity increased from 1.0 m/s in the healthy case (0% malfunction) to 1.85 m/s for the most severe one (100% malfunction) (+85%). Moreover, the flow direction changed from passing through the three orifices (one central and two laterals) in the healthy model to mainly lateral flow through the upper orifice in the completely closed leaflet case. In Fig. 3, for $Q=7$ L/min, the maximum velocity increased from 1.36 m/s in the healthy case (0% malfunction) to 2.63 m/s for the most severe one (100% malfunction) (+ 93%). Furthermore, it can be noticed on Fig. 4 that the flow is becoming more complex. The coherent structures (vortex structures) downstream of the valve were depicted using λ_2 criterion [12]. In the healthy model, two vortices shed from the trailing edges of both leaflets and other two ring-like vortices formed in the sinus area. This flow configuration is in agreement with the results of Ge et al. [9]. When the percentage of malfunction severity is increased, the flow downstream of the valve became more vortical with a significant increase in the number of small and large scale vortices. Moreover, a recirculation zone was created behind the

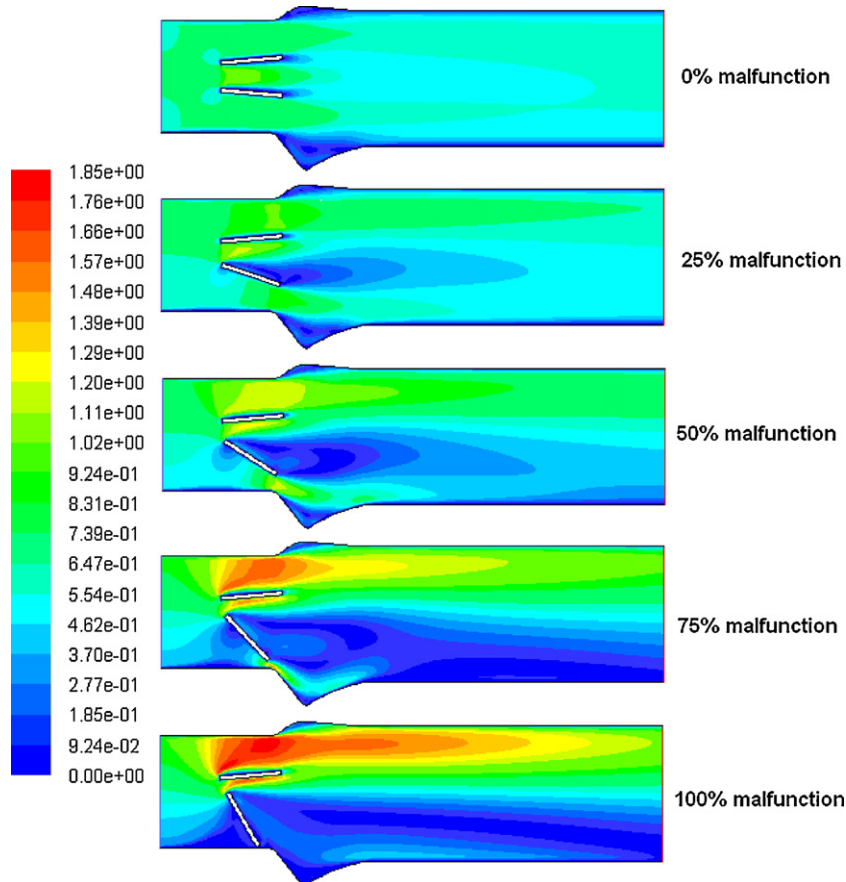


Fig. 2. Velocity magnitude (m/s) contours for different percentages of malfunction at $Q=5$ L/min.

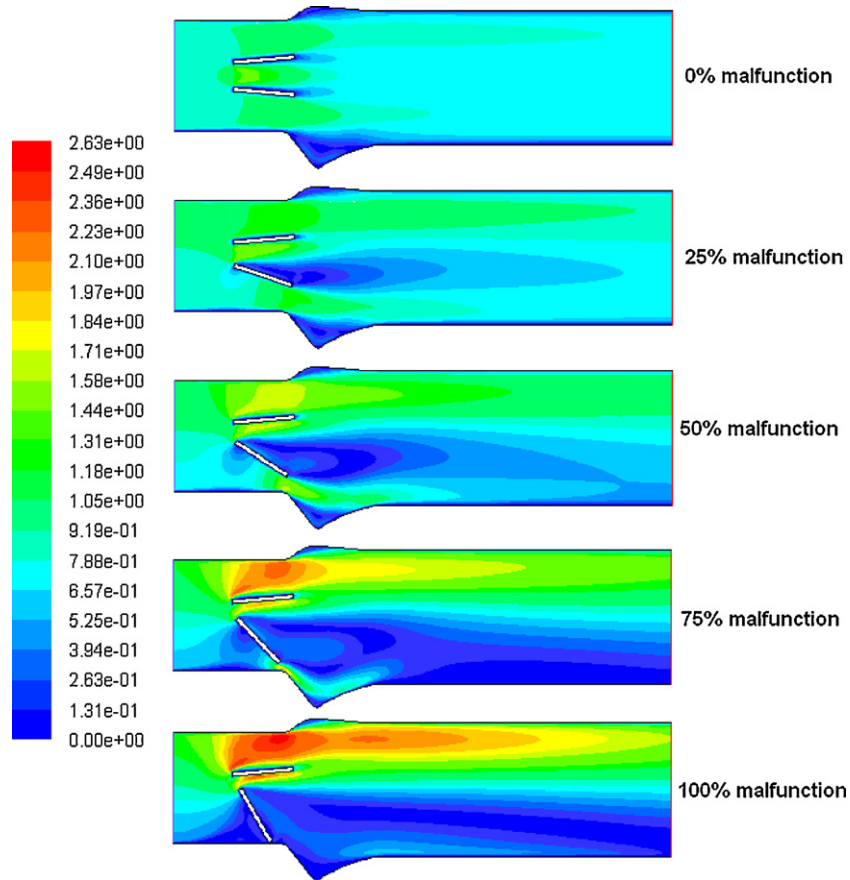


Fig. 3. Velocity magnitude (m/s) contours for different percentages of malfunction at $Q = 7 \text{ L/min}$.

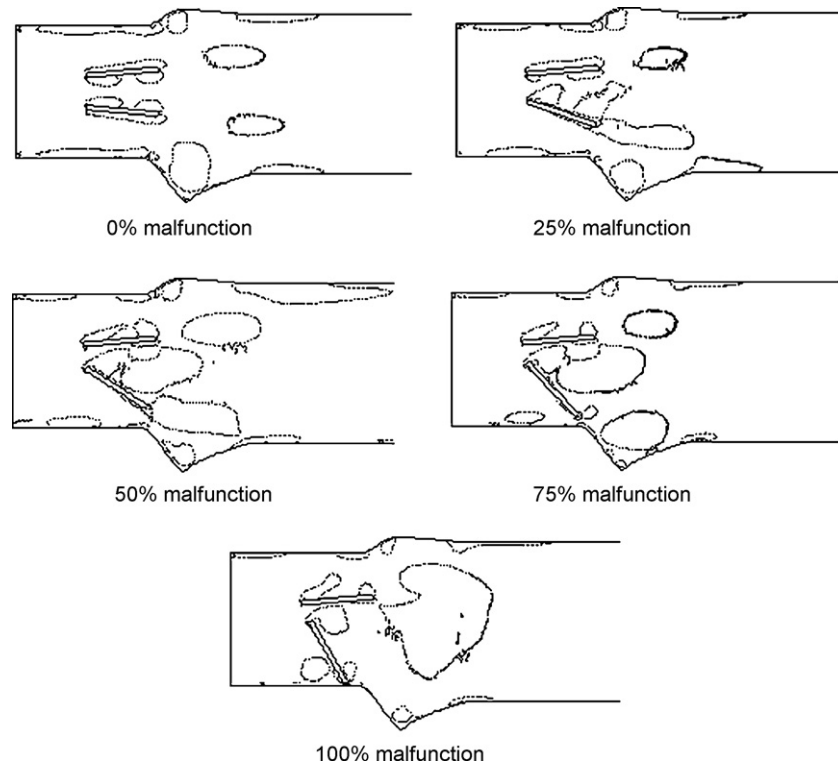


Fig. 4. Coherent structures downstream of a normal and a defective mechanical valve for 7 L/min (using the λ_2 criterion).

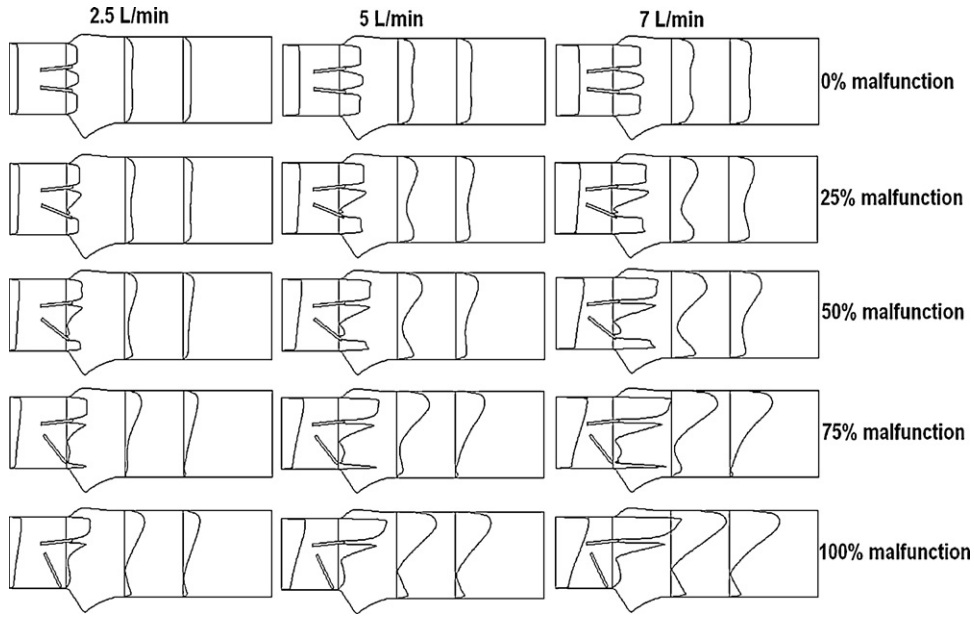


Fig. 5. Velocity profiles at the inlet, valve section, 1D downstream of the valve and 2D downstream of the valve for different percentages of malfunction and different flow rates.

defective valve especially in the case of completely defective valve.

Fig. 5 shows the velocity profiles at inlet section, valve section, 1D downstream of the valve and 2D downstream of the valve for different flow rates and valve malfunctions.

In the healthy model, the velocity profiles are in good agreement with the experimental data obtained by Grigioni et al. [7] on a St. Jude 19 mm valve, as shown on Fig. 6. For the defective valve, it is important to notice that applying a flat velocity profile few diameters upstream from the valve as an inlet condition for the numerical simulations is not realistic, since the flow is disturbed well before reaching the defective valve, this should also be the case for other obstacles such as a subaortic stenosis [13].

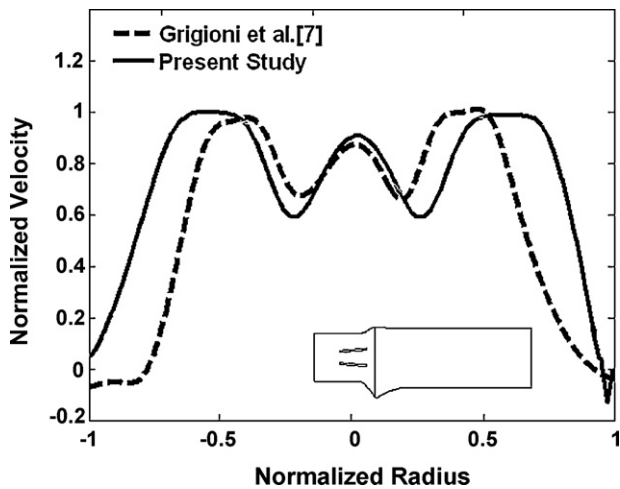


Fig. 6. Comparison between the normalized velocity profile at 7 mm downstream of the valve obtained experimentally by Grigioni et al. [7] for a St. Jude 19 mm mechanical valve and current numerical simulations.

Fig. 7 shows the position of the maximal velocity for 5 and 7 L/min, respectively for different percentages of valve malfunction. During Doppler echocardiography the probe is usually aligned with the valve to let the ultrasound wave beam to pass through the central orifice as the maximum velocity is expected to be at that position. However, from Fig. 5, this hypothesis seems to be applicable only for healthy or slightly defective valve (25% malfunction). On the contrary, the maximum velocity position started to shift to the lateral side when the severity of valve malfunction increases over 50%.

Fig. 8 shows the difference between average velocity and maximum velocity values for different flow rates and different percentages of valve malfunction. The deviation percentage was independent of flow rates and was a function of the percentage of malfunction. The maximum deviation was (132.3%). As a consequence, the assumption of a flattened velocity profile downstream of the valve, as used to determine the effective orifice area by Doppler echocardiography, is not applicable for a defective valve.

3.2. Transvalvular pressure gradient

Figs. 9 and 10 show the simulated Doppler echocardiographic transvalvular pressure gradient (TPG_{Dop}) obtained using the simplified Bernoulli equation ($TPG_{Dop} = 4V^2$); where: TPG_{Dop} is the transvalvular Doppler pressure gradient (mmHg) and V is the maximal velocity (m/s) (supposed to be at the vena contracta downstream of the valve).

TPG_{Dop} in Fig. 9 was determined based on the maximal velocity at the center line of the model. The maximum TPG_{Dop} was 11.93 mmHg for $Q = 7 L/min$ and 100% malfunction.

In Fig. 10, TPG_{Dop} was determined, now, using the maximal velocity in the entire field, simulating a conical ultra-

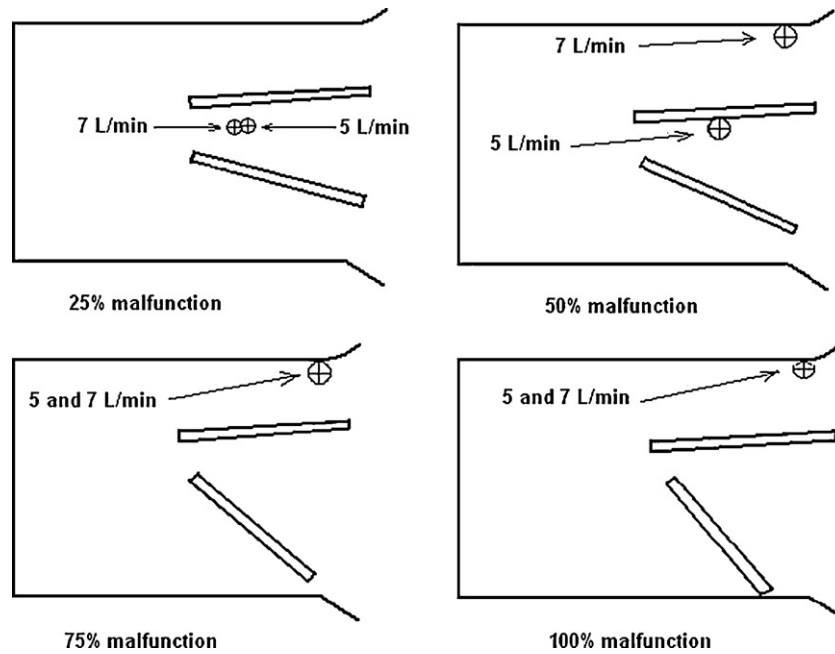


Fig. 7. Maximum velocity position at $Q = 5$ and 7 L/min for different percentages of valve malfunction.

sound beam. The maximum TPG_{Dop} was, in this case, 27.56 (mmHg) for $Q = 7$ L/min and 100% malfunction.

Fig. 11(a and b) shows the transvalvular pressure gradient, as measured by catheterization (TPG_{Cat}), for different percentages of valve malfunction and different flowrates. TPG_{Cat} was simulated using the difference between the average pressure at the inlet section of the model and the average pressure at a section located one diameter (1D) downstream of the valve on (Fig. 11 a) and a section located two diameters (2D) downstream of the valve on (Fig. 11 b). The TPG_{Cat} 1D downstream of the valve (Fig. 11 a) was 16.38 mmHg and 14.99 mmHg 2D downstream of the valve (Fig. 11 b) ($Q = 7$ L/min and 100% malfunction).

The difference between TPG_{Dop} and TPG_{Cat} is a manifestation of pressure recovery phenomenon. Interestingly, the discordance between TPG_{Dop} and TPG_{Cat} (distance to the identity line) is reduced with the increase in valve malfunction (Fig. 12). This is in agreement with the previous in vitro study performed by Baumgartner et al. [5] and can be explained by a more important energy loss downstream of the valve induced by a more severe malfunction.

3.3. Reynolds turbulent shear stress (TSS)

Figs. 13 and 14 show Reynolds turbulent shear stress in the entire field for 5 and 7 L/min, respectively. Five different

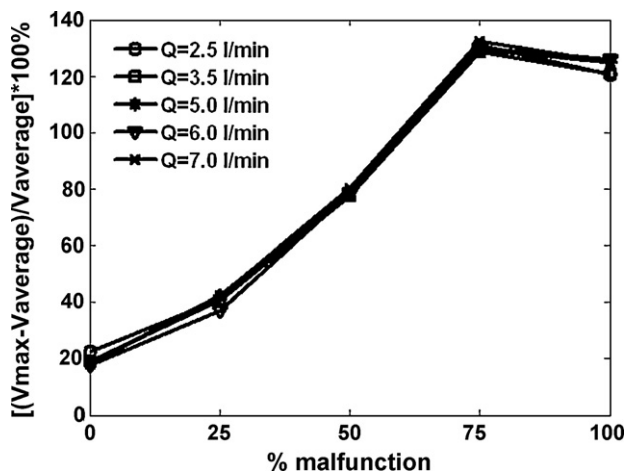


Fig. 8. The percentage of deviation between the maximal velocity (V_{max}) and the average velocity at 1D downstream of the valve for different percentages of valve malfunction and different flow rates.

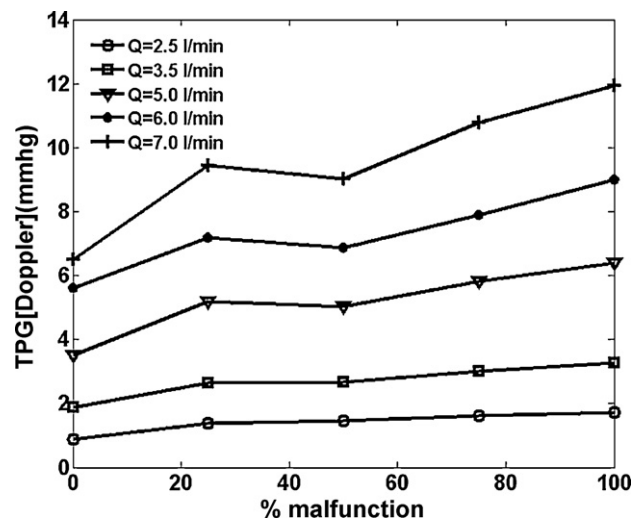


Fig. 9. Doppler transvalvular pressure gradient using the maximum velocity through the center line.

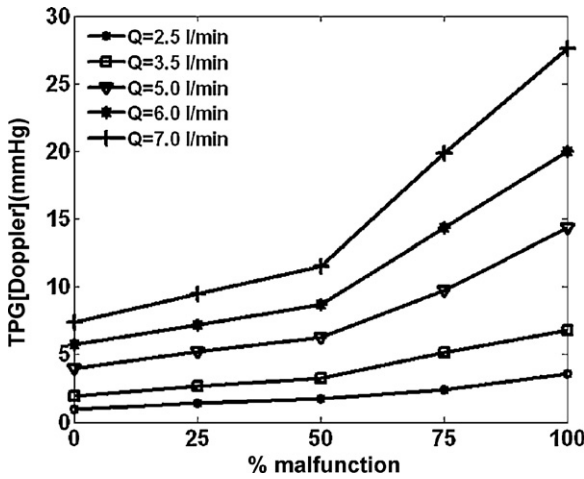


Fig. 10. Doppler transvalvular pressure gradient using the maximum velocity through the entire field.

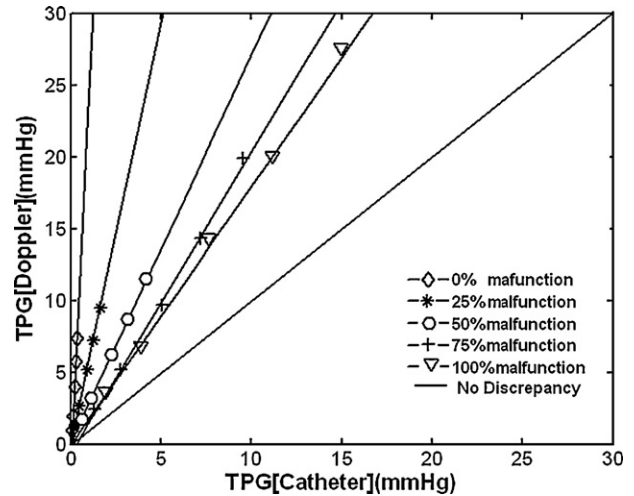


Fig. 12. Correlation between Doppler transvalvular pressure gradient and catheter transvalvular pressure gradient.

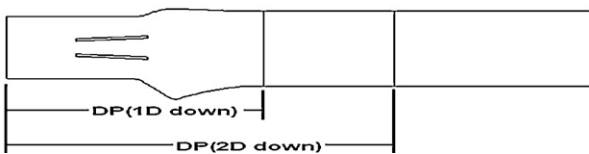
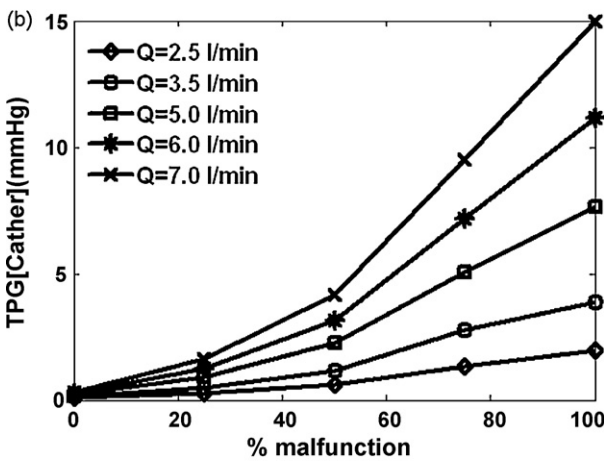
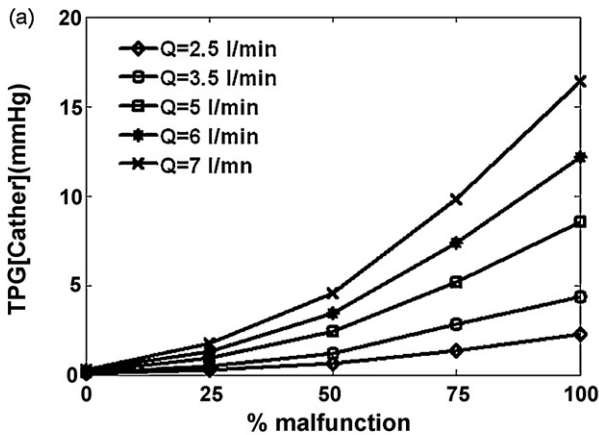


Fig. 11. Catheter transvalvular pressure gradient; (a) 1D downstream of the valve and (b) 2D downstream of the valve.

cases of malfunction have been considered for each flowrate. The TSS was obtained as [9]:

$$TSS = -\overline{\rho u'v'} = \mu_t \left(\frac{\partial u}{\partial y} + \frac{\partial v}{\partial x} \right)$$

where ρ the blood density (kg/m^3), u is the axial velocity (m/s), v is the radial velocity (m/s) and μ_t is turbulent viscosity kg/m s . In healthy valve, the maximum TSS value was around 32 and 56 Pa for $Q=5 \text{ L/min}$ ($Re=4075$) and $Q=7 \text{ L/min}$ ($Re=5708$), respectively. The TSS magnitude obtained in this study was in an over all agreement with Ge et al. [9] and Liu at al. [10]. Ge et al. obtained a maximal TSS value around 53 Pa at $Re=6000$ and for an inner diameter=20.4 mm using Unsteady Reynolds-averaged Navier-Stokes (URANS) approach. Moreover, Liu et al. found a maximal TSS value around 51 Pa for a cardiac output of 5 L/min, a heart rate of 70 beats/min and a systolic period 340 ms ($Re \sim 6500$) and for inner diameter=22 mm using Laser-Doppler Anemometry (LDA) measurements.

For both flowrates ($Q=5$ and 7 L/min) the maximum TSS was observed when the leaflet was completely closed (100% malfunction). The maximum TSS were 122 and 205 Pa for $Q=5$ and $Q=7 \text{ L/min}$, respectively. TSS was dominant in the wake of the leaflet, close to the trailing edge of each leaflet and the lower sinus region. As the percentage of malfunction increased, the dominant regions for the TSS started to be shifted towards the upper side of the valve and through the central orifice until the malfunction reached 100%; then, TSS had its highest value around the upper side of the normal leaflet.

4. Discussion

4.1. Boundary conditions

In general, the assumption of a flat profile (or a constant velocity) is commonly used as an inlet condition in steady and

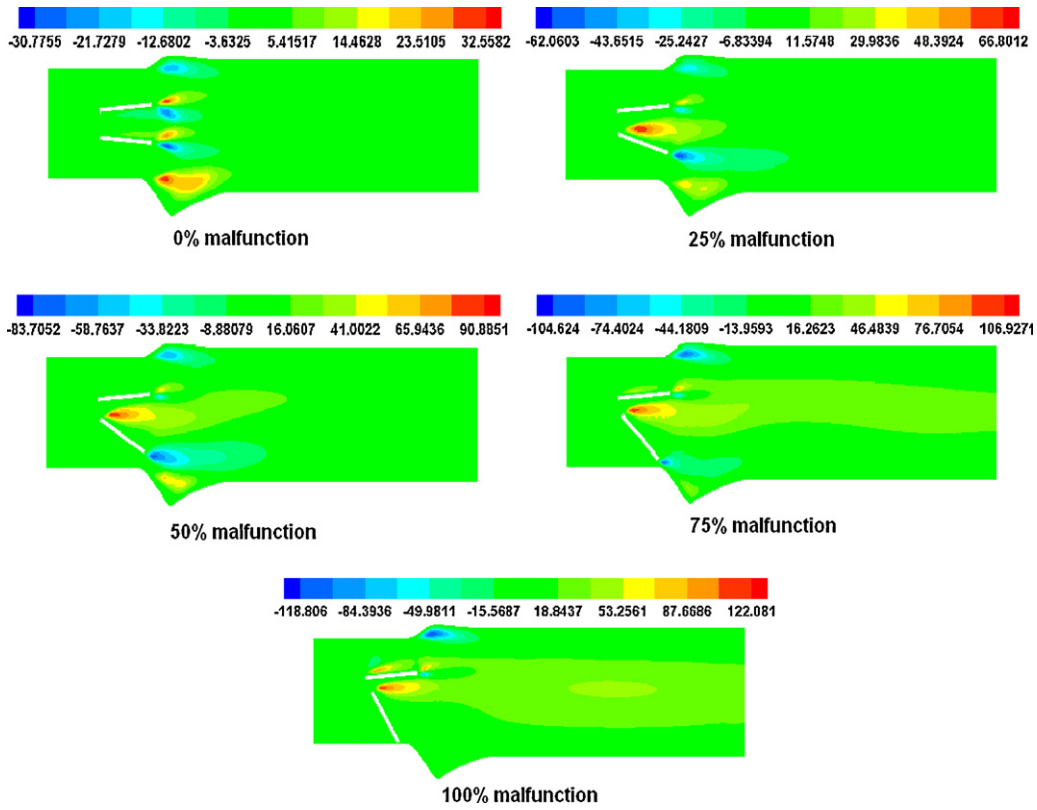


Fig. 13. Turbulent shear stress (Pa) at $Q = 5$ L/min for different percentages of valve malfunction.

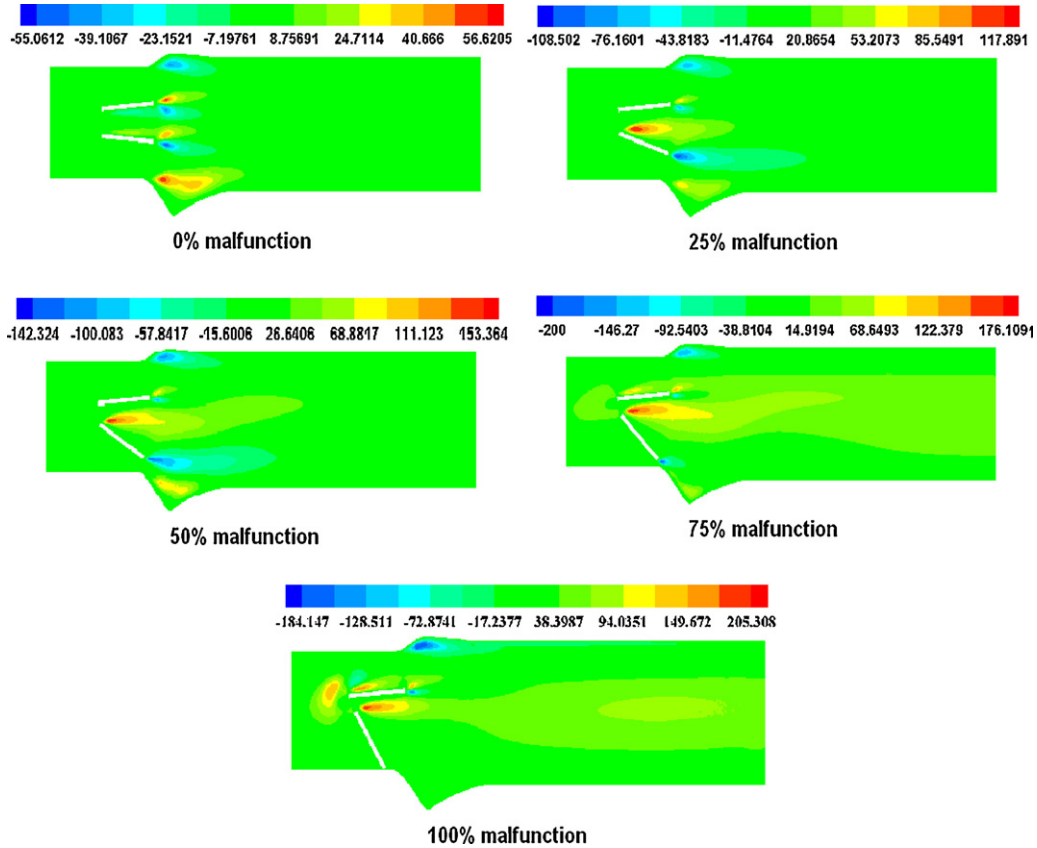


Fig. 14. Turbulent shear stress (Pa) at $Q = 7$ L/min for different percentages of valve malfunction.

unsteady investigations of the flow through native and prosthetic valves [8,14]. Although this assumption is reasonable in healthy models, it seems to be questionable for defective mechanical valves. Indeed, the velocity profile upstream from the valve is highly dependent upon the percentage of valve malfunction or the presence of any obstruction to the flow such a subaortic stenosis [13]. Therefore, it is more realistic to use the pressure difference between the inlet and outlet sections especially when simulating defective valve models. Furthermore, the weakness of the flattened assumption in defective mechanical heart valves raises a question concerning the precision of flow rate determination using pulsed wave Doppler upstream from the valve.

4.2. Diagnosis techniques for mechanical heart valve malfunction

4.2.1. Current existing techniques

Doppler echocardiography is currently the preferable method to investigate the performance of prosthetic valves. However, in more than 35% of cases, Doppler echocardiography alone was unable to detect a valve malfunction despite a significant leaflet restriction; this phenomenon is called “Doppler silent prosthetic valve thrombosis” [17]. This is due to different aspects related to both Doppler echocardiography and MHV design. Indeed, (1) the design of bileaflet MHV allows a quasi-normal flow when only one leaflet is blocked. As a consequence, patients with valve malfunction are usually asymptomatic; (2) Doppler echocardiography usually does not allow a clear visualization of the leaflets; (3) It is difficult to detect a valve malfunction using traditional Doppler echocardiographic parameters due to their flow dependence (transvalvular pressure gradients), pressure recovery phenomenon [18], and a wide variation among Doppler-derived parameters even for the same valve. For

this reasons, Aoyagi et al. [19] and Montorsi et al. [17] recommended that Doppler echocardiography should be used with another technique (such fluoroscopy or cineradiography). Indeed, Montorsi et al. showed that the concomitant use of fluoroscopy and Doppler echocardiography allow a correct diagnosis of a valve dysfunction in 85% of patients.

However, the main limitation associated with the above mentioned methods (fluoroscopy and cineradiography) is that the patient is exposed to X-rays. Hence, MRI can be used as a safer alternative to fluoroscopy and cineradiography. But unfortunately, despite the considerable developments in MRI techniques, mainly in phase contrast MRI, no studies have investigated yet its potential to detect and to evaluate MHV dysfunctions. Hence, the results of these numerical simulations can provide clinicians with some indications on what parameter can be used to detect MHV dysfunction.

4.3. Proposed diagnosis techniques

4.3.1. Doppler echocardiography

Fig. 15 shows the ratio between the increase in TPG_{Dop} and the increase in flow rate for different percentages of valve malfunction. The flow rate difference was taken for three cases; 5 L/min, 6 L/min and 7 L/min, simulating a normal case and an increase in flow rate induced by dobutamine injection. In the healthy valve this ratio was less than 2 for the all cases. Between 25 and 50% malfunction, the ratio increased slightly up to 3. Then, for higher malfunctions, the ratio increased rapidly to reach a maximal value between 5.5 and 7.5 for 100% of malfunction. This ratio can be a very interesting parameter to early detect a valve malfunction, when the transvalvular flow rate can be safely increased in patients.

4.3.2. Magnetic resonance imaging

Magnetic resonance imaging is currently one of the most promising techniques in cardiology and also in fluid mechanics [20]. In cardiology, MRI does not allow the visualization of valve leaflets, it allows, however, using phase contrast, the measurement of the velocity field upstream and downstream of normal, stenosed and prosthetic valves. Currently, phase contrast MRI is mainly used to evaluate the same parameters as the ones used by Doppler echocardiography (transvalvular pressure gradient, effective orifice area, . . .). They are, therefore, subject to the same limitations. Phase contrast MRI is mainly used, in this case, for a validation purpose. In the present work a new parameter extracted from the measurement of the velocity profile downstream of the valve has been introduced to detect any deviation from the standard velocity profile found in bileaflet MHV. Indeed, the results (Fig. 16) show that a velocity ratio (lateral/central) higher than 1 can be an indication of a valve malfunction. The important point to notice is that this parameter needs only one measurement and it is flow independent and does not need any information regarding the velocity in the LVOT (contrary to applying the continuity equation). Furthermore, this ratio is not sensitive

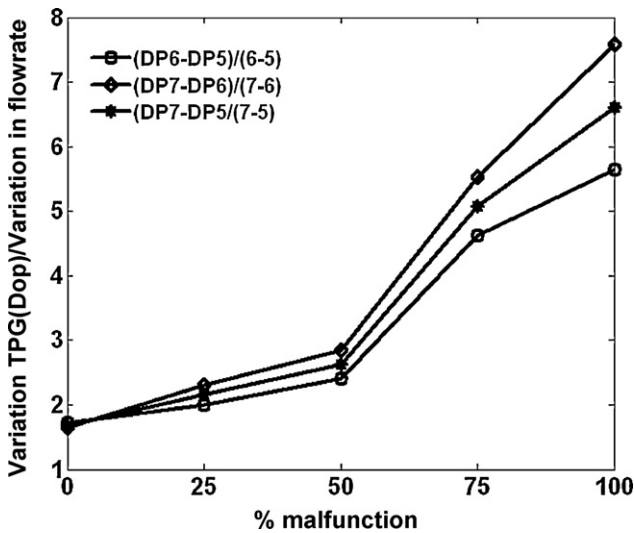


Fig. 15. Variation in Doppler transvalvular pressure gradient over the variation in flow rate for different percentages of valve malfunction (TPG_{Dop} is based on the maximal velocity in the entire field).

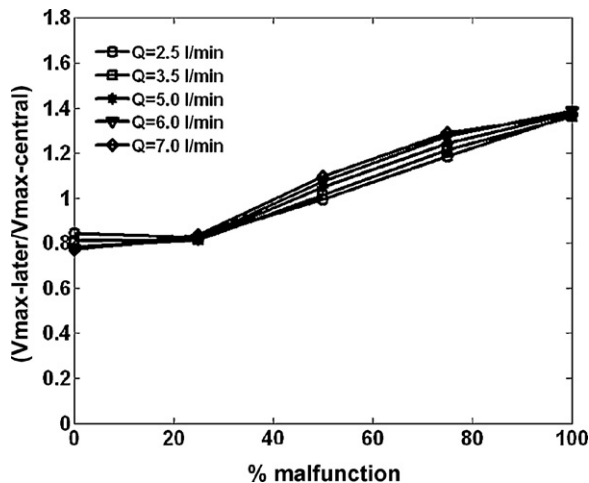


Fig. 16. Ratio between the maximal lateral jet velocity and the maximal central jet velocity for different flow rates and valve malfunctions.

to the choice of the encoding velocity and its magnitude should correlate with the percentage of valve malfunction.

4.3.3. Clinical complications

The non-physiological flow induced by the presence of the defective mechanical valve is responsible of a significant increase in Reynolds shear stress level, as a consequence, this might lead to platelet activation and red blood cells damage. Platelet activation is the major vector for thrombus formation in healthy mechanical heart valves and this activation occurs at lower shear stress than the ones required for blood hemolysis. A TSS magnitude of 400 N/m^2 and exposure time of 1 ms, are commonly used as thresholds for hemolysis [15], however, many studies have given different other values [16]. In this study, the TSS was elevated around four times in the case of 100% malfunction compared to healthy case. Adding to that, in the defective valve cases more small and large scale vortices were formed downstream of the valve which could increase red blood cells residential time in the relatively high TSS region. This will potentially lead to a significant platelet activation and thrombus formation. However, it should be noted that other parameters (other than TSS and exposure time) might play a significant role in platelet activation and blood hemolysis, such: shear exposure history, temperature, concentration of red blood cells and plasma components [11].

5. Limitations of the study

The realistic flow downstream of a mechanical heart valve is three-dimensional unsteady with fluid-structure interaction. However, in the present study the flow has been simulated as two-dimensional under steady state conditions. This can be justified by the fact that clinical parameters are usually phase-averaged parameters (mean transvalvular pressure gradient, effective orifice area) or measured exactly at the peak of the systolic phase (maximal transvalvular

pressure gradient), and the objective of this work is to introduce non-invasive parameters allowing an early diagnosis of mechanical heart valves malfunction.

Further in vitro and in vivo studies should allow validating these parameters under realistic conditions and estimating their accuracy. However, following the in vivo results obtained by Chafizadeh and Zoghbi [21] an error ranging between 6 and 18% for the Doppler echocardiographic parameters is expected in vivo. Under these conditions, it will be difficult to accurately diagnosis a MHV malfunction with a severity under 50%.

6. Conclusion

In the present study, the flow dynamics through a defective mechanical valve under steady state conditions, as a first approach, has been investigated. Discrepancies between Doppler echocardiographic and catheter transvalvular pressure gradients and the failure in the detection of mechanical valve malfunctions were clarified. Furthermore, two potential non-invasive methods, using Doppler echocardiography and magnetic resonance imaging, were proposed for an early detection of mechanical valve malfunction. The effect of such valve malfunction on blood components has also been investigated, and it appeared that it has a significant impact on platelet activation and, as a consequence, on thrombus formation.

Finally, more experimental and numerical studies on defective mechanical heart valves need to be conducted to give a clear idea about the blood hemodynamics and to improve the proposed diagnostic techniques to help clinicians to take the optimal decision.

Acknowledgements

The authors gratefully acknowledge the kind help of Drs. Pibarot and Gaillard. This work is supported by National Sciences and Engineering Research Council of Canada (NSERC Discovery grant 343165-07).

Conflict of interest statement

There is no conflict of interest.

References

- [1] Yoganathan AP, He Z, Jones SC. Fluid mechanics of heart valves. *Annu Rev Biomed Eng* 2004;6:331–62.
- [2] Sakamoto Y, Hashimoto K, Okuyama H, Ishii S, Shingo T, Kagawa H. Prevalence of pannus formation after aortic valve replacement: clinical aspects and surgical management. *J Artif Organs* 2006;9(3):199–202.
- [3] Baumgartner H, Khan S, DeRobertis M, Czer L, Maurer M. Discrepancies between doppler and catheter gradients in aortic prosthetic valves

- in vitro: a manifestation of localized gradients and pressure recovery. *Circulation* 1990;82:1467–514.
- [4] Montorsi P, Cavretto D, Alimento M, Muratori M, Pepi M. Prosthetic mitral valve thrombosis: can fluoroscopy predict the efficacy of thrombolytic treatment? *Circulation* 2003;108:79–84.
- [5] Baumgartner H, Schima H, Kuhn P. Effect of prosthetic valve malfunction on the doppler-Catheter gradient relation for bileaflet aortic valve prostheses. *Circulation* 1993;87:1524–4539.
- [6] Reul H, Vahlbruck A, Giersiepen M, Schmitz-Rode TH, Hirtz V, Effert S. The geometry of the aortic root in health, at valve disease and after valve replacement. *J Biomechanics* 1990;23(2):181–219.
- [7] Grigioni M, Daniele C, D'Avenio G, Barbaro V. The influence of the leaflets' curvature on the flow field in two bileaflet prosthetic heart valves. *J Biomechanics* 2001;34:613–21.
- [8] Ge L, Jones SC, Sotiropoulos F, Healy TM, Yoganathan AP. Numerical simulation of flow in mechanical heart valves: grid resolution and the assumption of flow symmetry. *J Biomechanical Eng* 2003;125:709–19.
- [9] Ge L, Leo H, Sotiropoulos F, Yoganathan AP. Flow in a mechanical bileaflet heart valve at laminar and near-Peak systole flow rates: CFD simulations and experiments. *J Biomechanical Eng* 2005;127:782–97.
- [10] Liu JS, Lu PC, Chu SH. Turbulence characteristics downstream of bileaflet aortic valve prosthesis. *J Biomechanical Eng* 2000;122:118–24.
- [11] Kameneva MV, Burgreen GW, Kono K, Repko B, Antaki JF, Umezo M. Effects of turbulent stresses upon mechanical hemolysis: experimental and computational analysis. *Am Soc Artif Internal Organs* 2004;50(5):418–23.
- [12] Jeong J, Hussain F. On the identification of a vortex. *J Fluid Mech* 1995;173:303–56.
- [13] Guivier C, Deplano V, Pibarot P. New insights into the assessment of the prosthetic valve performance in the presence of subaortic stenosis through a fluid-structure interaction model. *J Biomechanics* 2007;40(10):2283–91.
- [14] Grigioni M, Daniele C, Gaudio CD, Morbiducci U, D'Avenio G, Barbaro V. Three-dimensional numerical simulation of flow through an aortic bileaflet valve in a realistic model of aortic root. *Am Soc Artif Internal Organs* 2005;51(3):176–83.
- [15] Sallam AM, N. Hwang HC. Human red blood cells hemolysis in a turbulent shear flow: contribution of reynolds shear stress. *Biorheology* 1984;21:783–97.
- [16] Lu PC, Lai HC, Liu JS. A Reevaluation and discussion on the threshold limit for hemolysis in a turbulent shear flow. *J Biomechanics* 2001;34:1361–4.
- [17] Montorsi P, Cavoretto D, Alimento M, Muratori M, Pepi M. Prosthetic mitral valve thrombosis: can fluoroscopy predict the efficacy of thrombolytic treatment? *Circulation* 2003;108(II):78–84.
- [18] Osman F, Ludman P, Steeds R. Carbomedics bi-leaflet aortic valve prosthesis: a sticky problem. *Heart* 2006;92(11):1644.
- [19] Aoyagi S, Nishimi M, Tayama E, Fukunaga S, Hayashida N, Akashi H, et al. Obstruction of St. Jude medical valves in the aortic position: a consideration for pathogenic mechanism of prosthetic valve obstruction. *Cardiovasc Surg* 2002;10(4):339–44.
- [20] Bonn D, Rodts S, Groenink M, Rafai R, Shahidzadeh-Bonn N, Coussot P. Some Applications of magnetic resonance imaging in fluid mechanics: complex flows and complex fluids. *Annu Rev Fluid Mechanics* 2008;40:209–33.
- [21] Chafizadeh ER, Zoghbi WA. Doppler echocardiographic assessment of the St. Jude Medical prosthetic valve in the aortic position using the continuity equation. *Circulation* 1991;83:213–23.